Available online at www.sciencedirect.com
SCIENCE DIRECT®
Journal of Sound and Vibration 282 (2005) 89–109
JOURNAL OF SOUND AND VIBRATION
www.elsevier.com/locate/jsvi

Control of suspension bridge flutter instability using pole-placement technique

S. Pourzeynali[a,*], T.K. Datta[b]

[a]*Department of Civil Engineering, Faculty of Engineering, The University of Guilan, Rasht, Iran*
[b]*Department of Civil Engineering, Indian Institute of Technology, Hauz Khas, New Delhi 110 016, India*

Received 30 June 2003; accepted 16 February 2004
Available online 27 October 2004

Abstract

The closed-loop state feedback control scheme by pole-placement technique, which is widely used in control literature, is applied to control the flutter instability of suspension bridges. When the mean wind speed U at the bridge site increases beyond the critical flutter wind speed, the real part of the dominant pole of the system is forced to a desired negative value by properly designing a state feed back gain matrix to control the flutter instability. The control force, which is expressed as a product of gain matrix and state vector in modal coordinates, is applied in the form of an active torsional moment in the middle of the bridge span. The values of the state variables are estimated by designing a full order observer system. The application of the control scheme for increasing the critical wind speed for flutter of suspension bridges is demonstrated by considering the Vincent Thomas Bridge as the numerical example. The efficiency of the method for controlling the bridge deck flutter is investigated under a set of parametric variations. The results of the numerical study show that the control scheme using pole-placement technique effectively brings down the divergent oscillation of the bridge at wind speeds greater than the critical wind speed for flutter, to almost zero value within few seconds.

1. Introduction

Long-span suspension bridges, due to their flexibility and lightness, are much prone to the flutter instability. Flutter is a wind-induced instability in the bridge deck at a critical wind velocity

*Corresponding author. Tel.: +98-131-4429112; fax: +98-131-6690271.
E-mail address: pourzeynali@guilan.ac.ir (S. Pourzeynali).

0022-460X/$ - see front matter © 2004 Elsevier Ltd. All rights reserved.
doi:10.1016/j.jsv.2004.02.048

leading to an exponentially growing response. The evaluation of flutter condition of suspension bridges is one of the most important phases in the design of these bridges.

In recent years, many researchers [1–12] have focused their attention on increasing the critical flutter wind speed of the cable-supported bridges using different types of control devices. Wilde et al. [10] proposed a passive aerodynamic control of flutter by adding two additional surfaces to generate stabilizing forces and by putting an additional pendulum to control the torsional motion. Other studies also have been carried out to control the critical flutter wind speed of long-span bridges using eccentric mass on the bridges [13–15]. In 2002, the authors [12] proposed a passive control of critical flutter wind speed of suspension bridges using a combined vertical and torsional tuned mass damper (TMD) system. The proposed TMD system has two degrees of freedom, which are tuned close to the frequencies corresponding to vertical and torsional symmetric modes of the bridge, which get coupled during flutter.

Even with these advances, challenges still exist in increasing the critical flutter wind speed by applying reasonable external devices such as active control force or passive control properties, and trying to find practical methods to control the flutter condition of these bridges. In particular, application of pole-placement technique for control of bridge vibration is much less compared to that of optimal control theory [16]. Meirovitch and Ghosh [17] used modal control for suppressing the suspension bridge flutter, but they essentially used optimal control theory in modal space. Since control of bridge flutter is associated with the problem of making the system stable from an unstable state, the pole-placement technique should find as good application for this problem.

In this paper, the closed-loop state feedback control method by pole-placement technique, which has been used for other control problems, is applied to stabilize the flutter instability condition of suspension bridges. For this purpose, the equation of motion of the system is obtained by multi-mode finite element modeling (beam element) of the bridge deck using consistent mass matrix. The consistent mass matrix and structural stiffness matrix are evaluated using energy approach, which duly considers the effects of suspended cables. The final controlled equation of motion of the system is obtained in states space in terms of the generalized modal coordinate vector. The control force w is considered proportional to the values of the state vector, which are estimated by designing a full-order observer system. The control scheme is applied to suppress the flutter instability of Vincent Thomas Bridge and its effectiveness for flutter control of suspension bridge is investigated for different mean wind speeds through a numerical study.

2. Assumptions

The following assumptions are made in the analysis:

1. All stresses in the bridge elements obey the Hooke's law, and therefore no material nonlinearity is considered.
2. The control force and the output of the system are considered as scalar quantities.
3. The initial dead load is carried by cables without causing any stress in the suspended structure.
4. Small defection theory is applied to obtain the dynamic equation of motion of the suspension bridge.

3. Equation of motion of the bridge

The equation of motion of the system is obtained by multi-mode finite element method in time domain using the energy approach and applying the Hamilton's principle. For this purpose, the entire bridge is discretized into two-dimensional beam elements, each consisting of two nodes at its ends. At each node four degrees of freedom, namely vertical displacement (q_1^v), bending rotations (q_2^v), torsional rotation (q_1^θ), and warping displacement (q_2^θ), as shown in Fig. 1, are considered.

The governing equation of motion for flutter can be written as

$$[\mathbf{M}]\{\ddot{\mathbf{x}}\} + [\mathbf{C}]\{\dot{\mathbf{x}}\} + [\mathbf{K}]\{\mathbf{x}\} = \{\mathbf{F}\} + [\mathbf{B}_1]w, \tag{1}$$

where [**M**] is the consistent mass matrix, [**C**] is the structural damping matrix, [**K**] is the structural stiffness matrix, [$\mathbf{B}_1$] is the ($4n \times 1$) input matrix showing the location at which the control force is applied, w is the scalar constant control force, {**F**} is the ($4n \times 1$) vector of aeroelastic forces, and

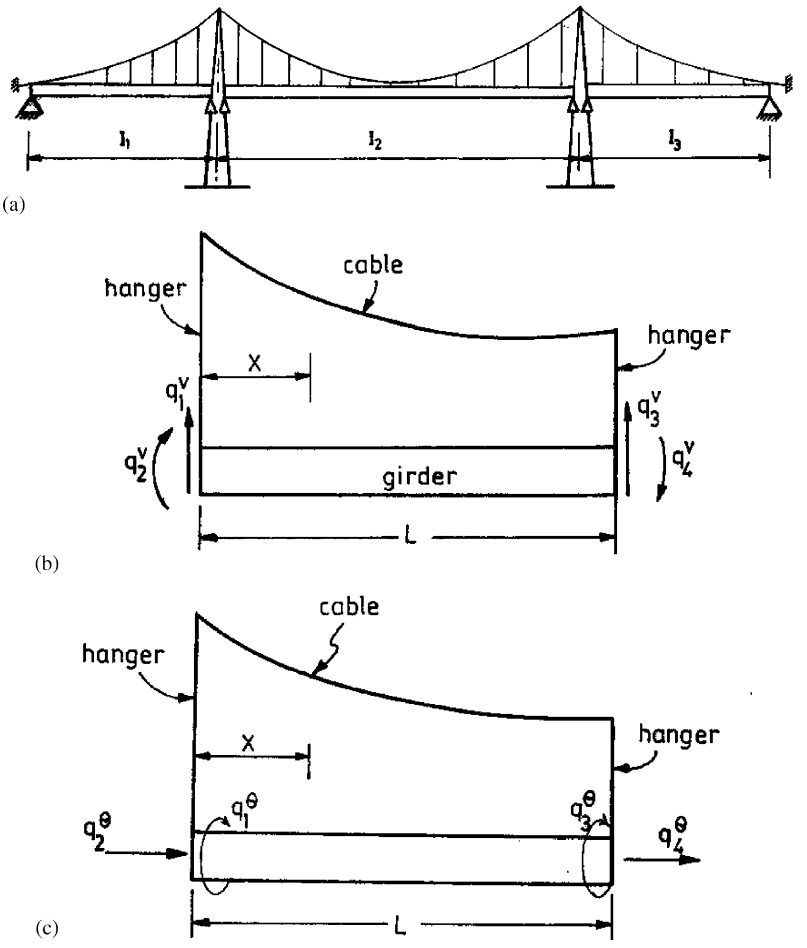

Fig. 1. (a) Suspension bridge model; (b) bridge element with vertical displacement; (c) bridge element with torsion.

$\{\mathbf{x}\}$ is the $(4n \times 1)$ response vector defined as follows

$$\{\mathbf{x}\} = \{x_1, x_2, \ldots, x_{4n}\}^{\mathrm{T}}_{1\times 4n} \tag{2}$$

in which n is the number of nodes along the total bridge length, x_i is the bridge response at ith degree of freedom. Note that the aeroelastic forces for bending rotation and warping degrees of freedom are zeroes.

The motion-dependent aeroelastic or self-excited forces acting per unit length of the bridge span as shown in Figs. 2(a) and (b) were presented by Scanlan et al. [18]. Meirovitch and Ghosh [17] used the expression given by Scanlan et al. [18] for investigating the flutter control of suspension bridges. Most complete version of the expression for the aeroelastic lift and moment forces were given by Jain et al. [19] and are used in the present study in the following form:

$$L_e = \frac{1}{2}\rho U^2 B' \left[kH_1^* \frac{\dot{h}}{U} + kH_2^* \frac{B'\dot{\theta}}{U} + k^2 H_3^* \theta + k^2 H_4^* \frac{h}{B'} \right], \tag{3a}$$

$$M_e = \frac{1}{2}\rho U^2 B'^2 \left[kA_1^* \frac{\dot{h}}{U} + kA_2^* \frac{B'\dot{\theta}}{U} + k^2 A_3^* \theta + k^2 A_4^* \frac{h}{B'} \right] \tag{3b}$$

in which ρ is the air mass density, U is the mean wind velocity, B' is the bridge deck width, $k = B'\omega/U =$ the reduced frequency, ω is the circular response frequency, H_i^* and A_i^*, $i = 1$ to 4 are the functions of k and are the experimentally determined flutter derivatives for the deck cross-section under investigation. Over dots indicate the time derivative. The flutter derivatives are obtained from wind tunnel tests on model bridge deck cross-sectional properties and are plotted as a function of the non-dimensional parameter k. For thin airfoil, analytical expressions are available for these derivatives. Experimental techniques to determine these derivatives are available in literature [20,21]. The details of the procedure for determining the flutter derivates used in the present investigation are given by Scanlan and Tomoko [20].

It is to be noted that the complete version of the aeroelastic expressions for the lift and moment forces contain two more terms which contain drag flutter derivatives associated with the lateral motion of the bridge deck. These two terms are neglected in the present study because they are not available for most of bridge sections reported in the literature. In one of the experimental studies

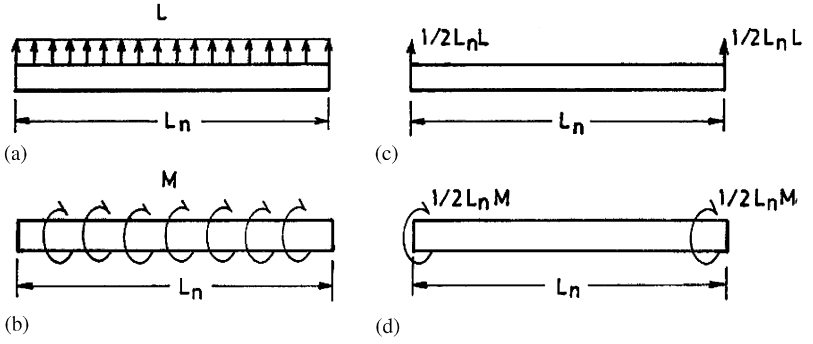

Fig. 2. Self-excited forces: (a) distributed vertical load; (b) distributed torsional moment; (c) lumped vertical load; (d) lumped torsional moment.

on model bridge cross-section Singh et al. [22] showed that there is a strong possibility of the dependence of lift on lateral (sway) motion. As a result, the lateral motion may significantly affect flutter wind speed if vertical–lateral or vertical–lateral–torsional mode of vibration predominantly governs the critical flutter wind speed. Since literature on the effect of lateral motion in modifying the critical wind speed for flutter of long span bridges in quantifiable terms is scanty, the present study considers only the vertical–torsional flutter condition for the control problem. If lateral motion is also included in the flutter problem, the pole placement technique can be easily extended for controlling such flutter condition.

The forces obtained by Eqs. (3a) and (3b) are considered to be constant along the element. In order to evaluate the aeroelastic force vector $\{\mathbf{F}\}$ in Eq. (1), the distributed aeroelastic forces are lumped at the element nodes as shown in Figs. 2(c) and (d). The mass and stiffness matrices in Eq. (1) are considered for double symmetric bridge deck and may be expressed as

$$[\mathbf{M}] = \begin{bmatrix} \mathbf{M}^V & \text{zeros} \\ \text{zeros} & \mathbf{M}^\theta \end{bmatrix}_{(4n\times 4n)}, \tag{4}$$

$$[\mathbf{K}] = \begin{bmatrix} \mathbf{K}^V & \text{zeros} \\ \text{zeros} & \mathbf{K}^\theta \end{bmatrix}_{(4n\times 4n)}, \tag{5}$$

where $\mathbf{M}^V$ and $\mathbf{K}^V$ are the mass and stiffness matrices, respectively in bending vibration, and $\mathbf{M}^\theta$ and $\mathbf{K}^\theta$ are those of the torsional vibration. Note that there is no modal coupling between the vertical and torsional modes of vibration in linear analysis for doubly symmetric bridge decks [23]. Using the total potential and kinetic energies of the bridge and applying the Hamilton's principle, the structural mass and stiffness matrices for vertical and torsional motions of the system can be evaluated [24,25]. The structural damping matrix $[\mathbf{C}]$ is assumed to be proportional to mass and stiffness matrices.

Using Eqs. (3a) and (3b) and lumping of the aeroelastic forces at the element nodes the $(4n \times 1)$ aeroelastic force vector $\{\mathbf{F}\}$ can be expressed in the form

$$\{\mathbf{F}\} = \frac{1}{2}\rho U^2 B' \left(\frac{k}{U}\right)[\mathbf{A}^F]\{\dot{\mathbf{x}}\} + \frac{1}{2}\rho U^2 B' k^2 [\mathbf{B}^F]\{\mathbf{x}\}, \tag{6}$$

where $\{\mathbf{x}\}$ is defined in Eq. (2), and matrices $[\mathbf{A}^F]$ and $[\mathbf{B}^F]$ are given in the Appendix A. Substituting Eq. (6) into Eq. (1), the final equation of motion can be expressed as

$$[\mathbf{M}]\{\ddot{\mathbf{x}}\} + [\mathbf{C}]\{\dot{\mathbf{x}}\} + [\mathbf{K}]\{\mathbf{x}\} = \frac{1}{2}\rho B'^2 \omega [\mathbf{A}^F]\{\dot{\mathbf{x}}\} + \frac{1}{2}\rho B'^3 \omega^2 [\mathbf{B}^F]\{\mathbf{x}\} + [\mathbf{B}_1]w. \tag{7}$$

It is convenient to solve problem of flutter control in modal space as carried out by Meirovitch and Ghosh [17]. By considering the displacement vector $\{\mathbf{x}\}$ in terms of modal matrix $[\mathbf{\Phi}]$ and generalized modal coordinate vector $\{\xi(t)\}$ as

$$\{\mathbf{x}\} = [\mathbf{\Phi}]\{\xi(t)\}_{m\times 1} \tag{8}$$

and using a standard modal transformation, the ith modal equation can be obtained as

$$\ddot{\xi}_i(t) + \sum_{j=1}^{m}\left[\left(2\zeta_i\omega_i\delta_{ij} - \frac{1}{2}\,\rho U^2 B'\,\frac{k}{U}\,\frac{d_{ij}}{\bar{m}_i}\right)\dot{\xi}_j(t)\right] + \sum_{j=1}^{m}\left[\left(\omega_i^2\delta_{ij} - \frac{1}{2}\,\rho U^2 B' k^2\,\frac{e_{ij}}{\bar{m}_i}\right)\xi_j(t)\right] = [\mathbf{\Phi}]^{\mathrm{T}}[\mathbf{B}_1]w, \quad i = 1, 2, \ldots, m, \tag{9}$$

$$\text{where } \delta_{ij} \text{ is the Kronecker delta function} = \begin{cases} 1, & i = j, \\ 0, & i \neq j, \end{cases} \tag{10}$$

m is the number of modes considered, $\bar{m}_i$ is the ith modal mass, and d_{ij} and e_{ij} are the elements of the matrices [**D**] and [**E**] defined as

$$[\mathbf{D}] = [\mathbf{\Phi}]^{\mathrm{T}}[\mathbf{A}^{\mathbf{F}}][\mathbf{\Phi}] \quad \text{and} \quad [\mathbf{E}] = [\mathbf{\Phi}]^{\mathrm{T}}[\mathbf{B}^{\mathbf{F}}][\mathbf{\Phi}]. \tag{11}$$

Eq. (9) can be written in a matrix form as

$$[\mathbf{I}]\{\ddot{\xi}(t)\} + [\mathbf{P}]\{\dot{\xi}(t)\} + [\mathbf{Q}]\{\xi(t)\} = [\mathbf{\Phi}]^{\mathrm{T}}[\mathbf{B}_1]w \tag{12}$$

in which [**I**] is the identity matrix of order m, [**P**] and [**Q**] are the square matrices of size $m \times m$ for which the elements can be defined as

$$P_{ij} = 2\zeta_i\omega_i\delta_{ij} - \frac{1}{2}\,\rho U^2 B'\,\frac{k}{U}\,\frac{d_{ij}}{\bar{m}_i}, \tag{13}$$

$$q_{ij} = \omega_i^2\delta_{ij} - \frac{1}{2}\,\rho U^2 B' k^2\,\frac{e_{ij}}{\bar{m}_i}. \tag{14}$$

Finally, by choosing the modal coordinates as the state variables, the state equation can be written in the standard state-space form as follows

$$\{\dot{\mathbf{z}}\} = [\mathbf{A}]\{\mathbf{z}\} + [\mathbf{B}]w \tag{15}$$

in which the $(2m \times 1)$ state vector $\{\mathbf{z}\}$ is defined as

$$\{\mathbf{z}\} = \begin{Bmatrix} \{\xi(t)\}_{m\times 1} \\ \{\dot{\xi}(t)\}_{m\times 1} \end{Bmatrix}_{2m\times 1}. \tag{16}$$

The state matrix [**A**], and the input matrix [**B**] are, respectively, given by

$$[\mathbf{A}] = \begin{bmatrix} [\mathbf{0}] & [\mathbf{I}] \\ -[\mathbf{Q}] & -[\mathbf{P}] \end{bmatrix}_{2m\times 2m}, \quad [\mathbf{B}] = \begin{bmatrix} [\mathbf{0}] \\ [\mathbf{\Phi}]^{\mathrm{T}}[\mathbf{B}_1] \end{bmatrix}_{2m\times 1}, \tag{17}$$

where [**0**] and [**I**] are the zero and identity matrices of order $m \times m$, respectively; and the other matrices previously are defined.

4. Design of control system by pole placement

According to the second method of Liapunov stability analysis, for a system represented by Eq. (15), the eigenvalues of the system need to be investigated. For this purpose, the eigenvalues of

the following equation is obtained:

$$\{\dot{\mathbf{z}}\} = [\mathbf{A}]\{\mathbf{z}\}. \tag{18}$$

If all eigenvalues of matrix [**A**] have negative real part, the system is asymptotically stable. Further, a necessary and sufficient condition for all eigenvalues to have negative real part is that they have determinant with positive coefficient of the leading terms of their characteristic polynomial. The eignvalues of the matrix [**A**] are called the poles of the original system. The stability of a linear closed-loop system can be determined from the location of the closed-loop poles in the complex s plane, in which s are the poles of the system. If any of these poles lie on the right half of the s plane, then the system is unstable. Therefore, closed-loop poles on the right half of s plane are not permissible in the usual linear control system. If all closed-loop poles lie to the left half of s plane, then the system is stable.

Whether a linear system is stable or unstable is a property of the system itself and does not depend on the input of the system. Thus, the problem of absolute stability can be solved readily by choosing no closed-loop poles on the right half of s plane, including the iω-axis. Mathematically, closed-loop poles on the iω-axis will yield oscillations, the amplitude of which is neither decaying nor growing with time. If dominant complex-conjugate closed-loop poles lie close to the iω-axis, the transient response exhibits excessive oscillations or it may be very slow. Therefore, to guarantee fast, yet well-damped, transient response characteristics, it is necessary that the closed-loop poles of the system lie in a particular region far away from the iω-axis. For a second-order closed-loop control system, it is shown [26] that the poles can be written as

$$s = -\zeta\omega_n \pm \mathrm{i}\omega_n\sqrt{1-\zeta^2} = -\zeta\omega_n \pm \mathrm{i}\omega_d, \quad \omega_d = \omega_n\sqrt{1-\zeta^2}, \quad \mathrm{i} = \sqrt{-1}, \tag{19}$$

where ζ is the damping ratio, ω_n is the undumped natural frequency (rad/s), and ω_d is the damped natural frequency. Without any loss of generality, for a multi-dof second-order closed-loop control system also, the poles can be written in the above form in terms of the modal damping ratio and natural frequency.

In suspension bridges at flutter condition ($U = U_f$, $\omega = \omega_f$, and $k = k_f$, where subscript f denotes the flutter condition), the damping of the dominant mode (mostly the torsional mode) is either zero or negative. Therefore, according to Liapunov's second method, the real part of dominant pole becomes either zero or positive, and makes the system unstable. It is shown [26] that if the system considered is completely state controllable, then poles of the closed-loop system may be placed at any desired location by means of state feedback through an appropriate state-feedback gain matrix. In the present study, the desired poles are chosen such that the real parts of all poles are negative. The procedure of designing the state feedback gain matrix in order to replace the poles of the system to desired values of $s_1 = \mu_1$, $s_2 = \mu_2, \ldots, s_n = \mu_n$, is given in the following.

Consider that the control force w in Eq. (15) is of the following form

$$w = -[\mathbf{K}_1]\{\mathbf{z}\} \tag{20}$$

in which w is the scalar value of the control force, $[\mathbf{K}_1]$ is the $1 \times (2m)$ state feedback gain matrix, and $\{\mathbf{z}\}$ is the state vector. Fig. 3 shows the block diagram of this closed-loop control system.

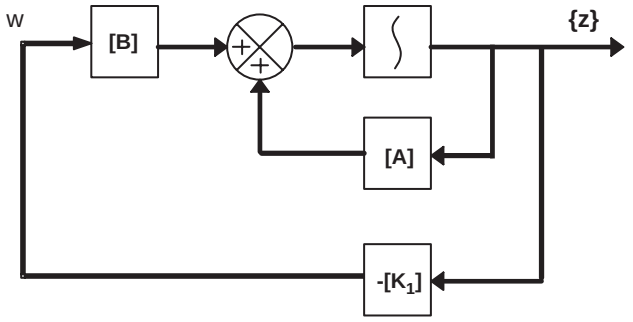

Fig. 3. Block diagram of closed-loop control system.

Substituting Eq. (20) into Eq. (15) gives

$$\{\dot{\mathbf{z}}\} = ([\mathbf{A}] - [\mathbf{B}][\mathbf{K}_1])\{\mathbf{z}\}. \tag{21}$$

If the matrix $[\mathbf{K}_1]$ is chosen properly, the matrix $([\mathbf{A}] - [\mathbf{B}] \times [\mathbf{K}_1])$ can be an asymptotically stable matrix and therefore, for any initial condition it is possible to make $\{\mathbf{z}(t)\}$ approach $\{\mathbf{0}\}$ as t approaches infinity. There are many active control schemes, which use the stability criterion for obtaining the gain matrix of the stable control system [27]. Also, detail discussions on the degree of stability are available in literature [27,28]. Here, pole placement technique is used for this purpose in which the eigenvalues of the matrix $([\mathbf{A}] - [\mathbf{B}]\,[\mathbf{K}_1])$ are the desired poles of the controlled system, which would replace the poles of unstable system. The necessary and sufficient condition for arbitrary pole placement to make all eigenvalues to have negative real part is that the rank of the controllability matrix $[\mathbf{H}]$, defined in Eq. (22), to be equal to the dimension of the matrix itself, i.e.,

$$[\mathbf{H}] = [\,\mathbf{B} \quad | \quad \mathbf{AB} \quad | \quad \ldots \quad | \quad \mathbf{A}^{n-1}\mathbf{B}\,], \tag{22}$$

where n is dimension of the matrices. Then, the state feedback gain matrix $[\mathbf{K}_1]$ can be written as

$$[\mathbf{K}_1] = [\alpha_n - a_n \quad \vdots \quad \alpha_{n-1} - a_{n-1} \quad \vdots \quad \cdots \quad \vdots \quad \alpha_2 - a_2 \quad \vdots \quad \alpha_1 - a_1][\mathbf{T}]^{-1}, \tag{23}$$

where $[\mathbf{T}]^{-1}$ is the inverse of the transformation matrix $[\mathbf{T}]$ given by

$$[\mathbf{T}] = [\mathbf{H}][\mathbf{W}] \tag{24}$$

and a_i's are coefficients of the characteristic polynomial

$$|s\mathbf{I} - \mathbf{A}| = s^n + a_1 s^{n-1} + \cdots + a_{n-1}s + a_n \tag{25}$$

and the coefficients α_i's are related to the desired poles $s_1 = \mu_1$, $s_2 = \mu_2, \ldots, s_n = \mu_n$, and can be obtained from the desired characteristic equation as

$$(s - \mu_1)(s - \mu_2)\cdots(s - \mu_n) = s^n + \alpha_1 s^{n-1} + \cdots + \alpha_{n-1}s + \alpha_n = 0. \tag{26}$$

Matrix [**W**] in Eq. (24) is given as

$$[\mathbf{W}] = \begin{bmatrix} a_{n-1} & a_{n-2} & \cdots & a_1 & 1 \\ a_{n-2} & a_{n-3} & \cdots & 1 & 0 \\ \vdots & \cdots & \cdots & \cdots & \cdots \\ a_1 & 1 & \cdots & 0 & 0 \\ 1 & 0 & \cdots & 0 & 0 \end{bmatrix}, \tag{27}$$

where a_i's are given by Eq. (26).

It is noted that for a given system, the matrix $[\mathbf{K}_1]$ is not unique, but depends on the desired closed-loop locations selected, which determine the decay of the response. In order to determine the gain matrix $[\mathbf{K}_1]$ for a given system, the response characteristics of the control system is to be studied for a number of cases and the best one is to be selected.

For calculating the gain matrix $[\mathbf{K}_1]$, the full-order state variables are needed. It is seen from Eq. (15) that the generalized modal coordinates are taken as the state variables for the problem. Since these state variables are not measurable, it is necessary to design a full-order observer system to estimate the values of state variables from the actually measured responses. These estimated values of the state variables are used in Eq. (20) for calculating the control force w.

5. Design of full-order observer system

Consider that a system with a single input w and a single output y is given by the following equations:

$$\{\dot{\mathbf{z}}\} = [\mathbf{A}]\{\mathbf{z}\} + [\mathbf{B}]w, \tag{28}$$

$$y = [\mathbf{C}_1]\{\mathbf{z}\}, \tag{29}$$

$$w = -[\mathbf{K}_1]\{\mathbf{z}\}. \tag{30}$$

Assume that, for this system the state $\{\mathbf{z}\}$ is to be approximated by the state $\{\tilde{\mathbf{z}}\}$ through an observer system for which the dynamic model is given by the following equation:

$$\{\dot{\tilde{\mathbf{z}}}\} = [\mathbf{A}]\{\tilde{\mathbf{z}}\} + [\mathbf{B}]w + [\mathbf{K}_e](y - [\mathbf{C}_1]\{\tilde{\mathbf{z}}\}), \tag{31}$$

where $[\mathbf{K}_e]$ is the observer gain matrix. It is noted that the last term in Eq. (31) is a correction term that involves the difference between the measured output y and the estimated output $[\mathbf{C}_1]\{\tilde{\mathbf{z}}\}$, and matrix $[\mathbf{K}_e]$ serves as a weighting matrix. Also, in the case of any difference between the matrices [**A**] and [**B**] of the actual system and those used in the observer model, the additional correction terms will reduce the effect of this difference. Fig. 4 shows the block diagram of the control system and the full-order state observer. Subtracting Eq. (31) from Eq. (28), an equation in terms of observer error vector $\{\mathbf{e}\}$ can be written as

$$\{\dot{\mathbf{e}}\} = [(\mathbf{A}] - [\mathbf{K}_e][\mathbf{C}_1])\{\mathbf{e}\}, \tag{32}$$

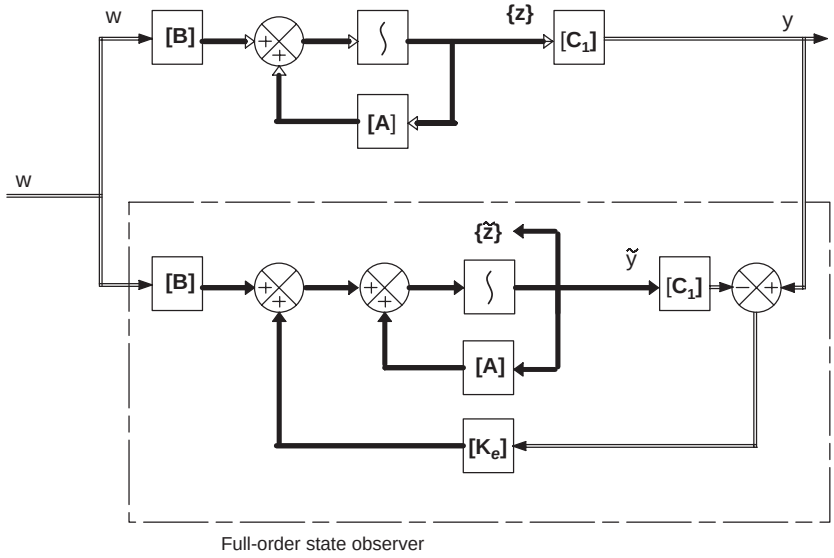

Fig. 4. Block diagram of control system with full-order observer system.

where

$$\{\mathbf{e}\} = \{\mathbf{z}\} - \{\tilde{\mathbf{z}}\}. \tag{33}$$

The dynamic behavior of vector $\{\mathbf{e}\}$ depends on the eigenvalues of the matrix $([\mathbf{A}] - [\mathbf{K}_e][\mathbf{C}_1])$. It means that if matrix $([\mathbf{A}] - [\mathbf{K}_e][\mathbf{C}_1])$ is a stable matrix, then the error vector $\{\mathbf{e}\}$ approaches to zero for any initial error $\{\mathbf{e}(\mathbf{0})\}$. Therefore, similar to the pole-placement technique, it is possible to calculate the $[\mathbf{K}_e]$ matrix such that the matrix $([\mathbf{A}] - [\mathbf{K}_e][\mathbf{C}_1])$ has the desired eigenvalues. By defining a dual system, the desired $[\mathbf{K}_e]$ matrix is evaluated. The details are given by Ogata [26].

The procedure (given in Sections 4 and 5) for the design of full-order observer system and determination of gain matrices $[\mathbf{K}_e]$ and $[\mathbf{K}_1]$ are explained for single input control force and single response out put. The procedure can be easily extended to multi-point control actions and multi-point response measurements. Multi-point control actions, which are same in magnitude and phase, can be accommodated by making the elements of location vector $\{\mathbf{B}_1\}$ as unity corresponding to locations where control forces are introduced. Accordingly, $[\mathbf{K}_1]$ or $[\mathbf{K}_e]$ row matrices are changed, but they can be generated using computer simulation without much difficulty. However, when multi-point input signals (control forces) are different in magnitude and phase, i.e., they form a vector quantity, the mathematical aspects of the pole placement scheme become complicated. In that event, the state feedback gain matrix is not unique because placement of the required number of closed-loop poles is not completely correlated to the system dynamics. It is possible to choose freely some other parameters that may change the gain matrix. The details of the treatment of multi-point input signal represented as a vector quantity is given by

Ogata [29]. Multi-point response measurements can be easily accommodated by modifying $[\mathbf{C}_1]$ matrix (Eq. (29)), elements of which are assembled from the mode shape matrix of the system represented by Eq. (15).

6. Equation of motion of the system with observer

The control force w as given by Eq. (20), should therefore be written as

$$w = -[\mathbf{K}_1]\{\tilde{\mathbf{z}}\}, \tag{34}$$

where $\{\tilde{\mathbf{z}}\}$ is the estimated value of the state vector. By combining Eqs. (8), (9), (12)–(14), and (21), the final state-space equation of the control system can be expressed as

$$\begin{Bmatrix} \dot{\mathbf{z}} \\ \dot{\mathbf{e}} \end{Bmatrix} = \begin{bmatrix} \mathbf{A} - \mathbf{B}\mathbf{K}_1 & \mathbf{B}\mathbf{K}_1 \\ 0 & \mathbf{A} - \mathbf{K}_e\mathbf{C}_1 \end{bmatrix} \begin{Bmatrix} \mathbf{z} \\ \mathbf{e} \end{Bmatrix}. \tag{35}$$

This control system is called observed-state feedback control system. Therefore, the design procedure of an observed-state feedback control system becomes a two-stage process. In the first stage, the state feedback gain matrix $[\mathbf{K}_1]$ and in the second stage, the state-observer gain matrix $[\mathbf{K}_e]$ is to be calculated.

7. Numerical study

As the numerical example, the Vincent Thomas Suspension Bridge located between San Pedro and Terminal Island in Los Angeles County, California is chosen.

The stiffening girder is assumed to be hinged at the ends in each span, and the cables are free to move at the tower top (i.e. roller type cable connection). The number of elements in the side spans, $N_1 = N_3$, is taken to be 11 elements, and those for the center span, N_2 is taken as 28 elements.

For this three-span suspension bridge, the structural data are taken from the literature [24,25]. Some of the structural data are given in the following:

(1) one center span $l_2 = 460\,\text{m}$; (2) two side spans $l_1 = l_3 = 155\,\text{m}$; (3) dead load of the bridge $\overset{*}{w} = 52438.020\,\text{N/(m-cable)}$; (4) cross-sectional area of one cable, $A_c = 0.0780\,\text{m}^2$; (5) moment of inertia of bridge deck for center span $I_2 = 0.7258\,\text{m}^4$, and for side spans $I_1 = I_3 = 0.7498\,\text{m}^4$.

The results of the free vibrational analysis (first 19 frequencies and first 6 mode shapes) are respectively shown in Table 1 and Fig. 5. In the figure, V and T refer to vertical and torsional respectively, and A and S refer to anti-symmetric and symmetric, respectively. It is seen that the first five modes correspond to the vertical mode of vibration. Note that free vibrational mode shapes are either purely vertical or purely torsional as it would be expected.

Table 1
Modal properties of Vincent Thomas Suspension Bridge

Mode no.	Frequency ω (rad/s)	Mode type	Modal mass ($\bar{m}$)
1	1.2324	V-AS	2459813.72
2	1.3743	V-S	2241151.36
3	2.1595	V-AS	1691846.37
4	2.1744	V-S	2835117.10
5	2.8710	V-S	2473230.58
6	3.1163	T-S	97988365.63
7	3.4215	V-AS	2587940.03
8	4.4124	T-AS	104389535.3
9	5.0012	V-S	2370506.36
10	6.68024	T-AS	71798615.43
11	6.7388	T-S	127314525.1
12	6.8351	V-AS	853012.18
13	6.8352	V-S	1021244.00
14	6.8791	V-AS	2460065.24
15	7.0556	T-S	90569439.11
16	9.1062	V-S	2441548.53
17	9.2418	T-AS	1098227534.8
18	11.6557	V-AS	2587889.91
19	11.9381	T-S	103285020.90

Note: T = torsional; V = vertical; S = symmetric; AS = anti-symmetric.

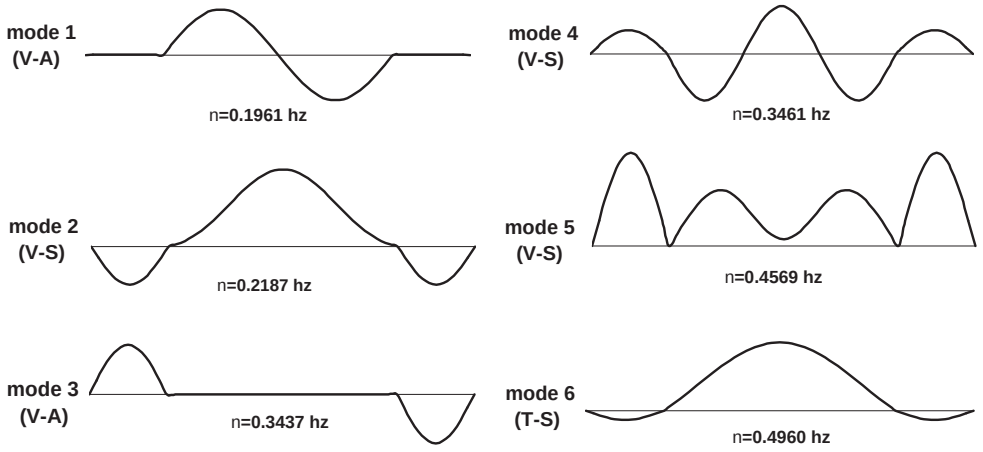

Fig. 5. First six free vertical and torsional vibrations mode shapes.

The approximate theoretical expressions for the flutter derivatives for the bridge deck may be written as [20]

$$\begin{aligned}
&A_1^* \simeq 0;\ H_1^* = -0.8y_1 \quad \text{for all } y_1,\\
&A_2^* = -0.1436\sin(0.5984y_1), \quad 0 \leqslant y_1 \leqslant 5.25,\\
&A_2^* = 0.08422y_1 - 0.4411, \quad 5.25 < y_1,\\
&H_2^* = 0, \quad 0 \leqslant y_1 \leqslant 5,\\
&H_2^* = 0.00582y_1^3 - 0.0121y_1^2 - 0.60252, \quad 5 < y_1,\\
&A_3^* = 0, \quad 0 \leqslant y_1 \leqslant 2,\\
&A_3^* = 0.2y_1 - 0.4, \quad 2 \leqslant y_1 \leqslant 6,\\
&A_3^* = 0.3y_1 - 1, \quad 6 < y_1,\\
&H_3^* = 0, \quad 0 \leqslant y_1 \leqslant 4,\\
&H_3^* = -0.011666y_1^3 + 0.11y_1^2 - 1.41334y_1 + 4.64003, \quad 4 < y_1
\end{aligned} \tag{36}$$

in which

$$y_1 = \frac{2\pi}{k}, \quad k = \frac{B'\omega}{U}.$$

Since the values of H_4^* *and* A_4^* for this bridge are not available, they are assumed to be negligible.

The flutter condition of this bridge is obtained by authors in another study [12]. It is observed that the 6th mode (i.e. the first symmetric torsional mode) is the predominant mode for the flutter condition. This mode gets coupled with the 2nd and 5th modes, which are the first and third vertical symmetric modes, respectively for the flutter condition. The contributions of the other modes in flutter occurrence are very less in comparison with these modes. Thus, consideration of first four modes for the flutter analysis is sufficient. Therefore, for further parametric studies first four modes are considered in the analysis. The flutter condition for this bridge, for a damping ratio of 0.8%, is calculated as $U_f = 55.52\,\text{m/s}$, $\omega_f = 2.9125$, and $k_f = 0.946$.

In order to perform the stability analysis, the responses of the bridge due to initial condition, for three different mean wind speeds, $U = 50\,\text{m/s}$, $U = U_f = 55.52\,\text{m/s}$ and $U = 60\,\text{m/s}$, are considered. The initial condition for the state variables $\{\mathbf{z}\}$ is considered as $\{\mathbf{z}_0\} = \{0, 0, 0, 0.05, 0, 0, 0, 1\}$.

Figs. 6 and 7 compare the results of the controlled and uncontrolled responses of the bridge at a mean wind speed $U = 50\,\text{m/s}$, which is less than the critical flutter wind speed for this bridge. Fig. 6 shows the vertical displacement, while Fig. 7 shows the torsional displacement of the bridge. As it can be seen from the figures, when U is less than U_f, the uncontrolled response of the bridge decays with time. The eigenvalues of state matrix [**A**] for this case is shown in Table 2. It is seen from the table that the real parts of all eigenvalues (poles of the system) are negative and therefore, the system is stable. In order to control the system the real part of the dominant pole, i.e. −0.0056, is replaced with a value of −0.08. The values of the other poles are kept the same as they were. It is seen from Figs. 6 and 7 that both vertical and torsional responses decay much faster and reach to almost zero value within a very short time. The control action needed to force the dominant pole of the system from −0.0056 to −0.08, is shown in Fig. 8. It is seen from the

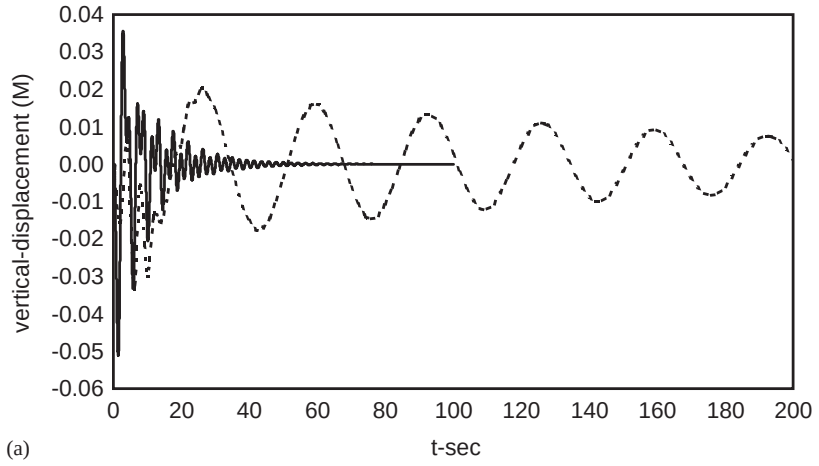

Fig. 6. Controlled and uncontrolled bridge vertical responses due to initial conditions at mean wind speed $U = 50\,\mathrm{m/s}$ (original ----, controlled —).

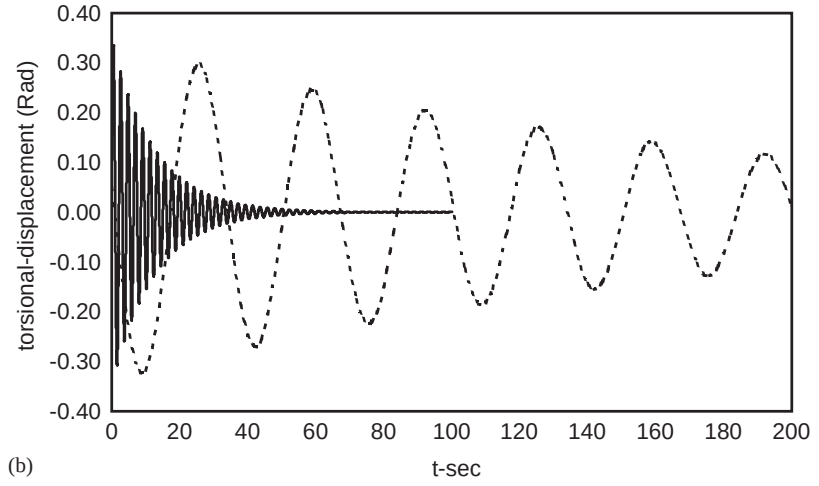

Fig. 7. Controlled and uncontrolled bridge torsional responses due to initial conditions at mean wind speed $U = 50\,\mathrm{m/s}$ (original ----, controlled —).

figure that very small control action is required to make the responses decay at a faster rate. Note that the applied control action is a torsional moment applied at the middle of the center span of the bridge. This is the case because the torsional mode of vibration practically governs the responses of the particular bridge as discussed before.

Comparison between the results of the controlled and uncontrolled responses of the bridge at flutter condition, i.e. $U = U_f = 55.52\,\mathrm{m/s}$; and at $U = 60\,\mathrm{m/s}$, which is more than the critical flutter wind speed, is shown in Figs. 9 and 10, respectively. It is seen from the figures that the

Table 2
Eigenvalues of the state matrix [**A**] in different cases

Case 1, $U = 50$ (m/s)	Case 2, $U = U_f = 55.52$ (m/s)	Case 3, $U = 60$ (m/s)
$-0.1434 + 1.3666i$	$-0.1581 + 1.3650i$	$-0.1699 + 1.3636i$
$-0.1434 - 1.3666i$	$-0.1581 - 1.3650i$	$-0.1699 - 1.3636i$
$-0.1554 + 2.8666i$	$-0.1700 + 2.8657i$	$-0.1819 + 2.8650i$
$-0.1554 - 2.8666i$	$-0.1700 - 2.8657i$	$-0.1819 - 2.8650i$
$-0.1498 + 2.1694i$	$-0.1645 + 2.1684i$	$-0.1763 + 2.1674i$
$-0.1498 - 2.1694i$	$-0.1645 - 2.1684i$	$-0.1763 - 2.1674i$
$-0.0056 + 2.9529i$	$-0.0001 + 2.9131i$	$+0.0047 + 2.8776i$
$-0.0056 - 2.9529i$	$-0.0001 - 2.9131i$	$+0.0047 - 2.8776i$

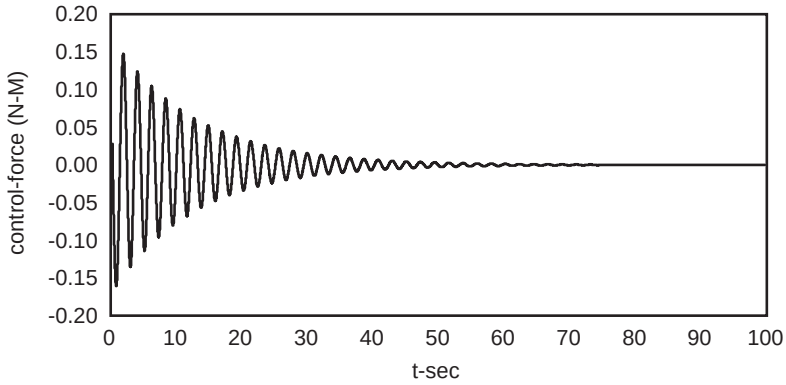

Fig. 8. Control force to reduce the bridge response at mean wind speed $U = 50\,\mathrm{m/s}$.

uncontrolled responses are sustained harmonic motion for flutter wind speed, while for wind speed greater than flutter speed (i.e. to up to 60 m/s) they diverge to infinity with increase in time. The eigenvalues of the state matrix [**A**] for these two cases are also shown in Table 2. It is seen from the table that the real part of the dominant pole, for the flutter condition is almost zero (-0.0001), while that for $U = 60\,\mathrm{m/s}$, it is positive ($+0.0047$). Therefore, the system is unstable for both cases. In order to control the response, the real parts of the dominant poles of both cases are changed to -0.08 keeping the values of other poles to remain the same as they were. Note that the value of -0.08 is selected by computer simulation in order to obtain a good controlled response. The elements of the state control feedback gain matrix [$\mathbf{K}_1$] for the above three cases are given in Table 3.

It is seen from the figures that the transient responses are brought to almost zero values within 50 s. Thus, the active control with a torsional moment at the middle of central span of the bridge can alleviate the flutter wind speed considerably.

Figs. 11 and 12 show the values of the active control forces, which are applied to the system for the above two cases. It is seen that the maximum values of the torsional moment required for the

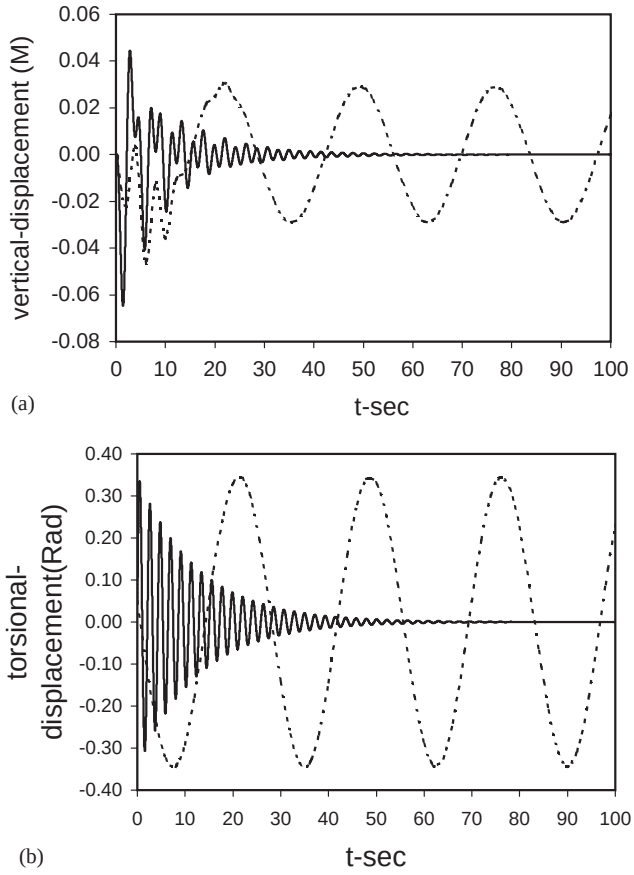

Fig. 9. Controlled and uncontrolled bridge responses due to initial conditions at mean wind speed $U = U_f = 55.52\,\mathrm{m/s}$ (original ----, controlled —).

two cases are not significantly different and are quite small. This indicates the effectiveness of the pole-placement technique to stabilize the flutter instability of the suspension bridges.

In order to design the full-order observer system, the poles of the observer are selected as $\{-1,-1,-1,-1,-6,-6,-6,-6\}$. These values are also chosen based on the computer simulation such that to make the speed of the state observer error around five times of the response control speed. Fig. 13 shows the variation of the error between the actual state variables and observed state variables versus time, for the case of $U = 50\,\mathrm{m/s}$. It is seen from the figure that after about 10 s, the values of the estimated variables approach to the actual variables. A similar behavior is observed for the other two cases of the wind speed. $[\mathbf{K}_e]$ for the three cases are also given in Table 3.

8. Conclusion

An efficient closed-loop state feed back control scheme using pole-placement technique is presented for active control of suspension bridge flutter. The control algorithm consists of

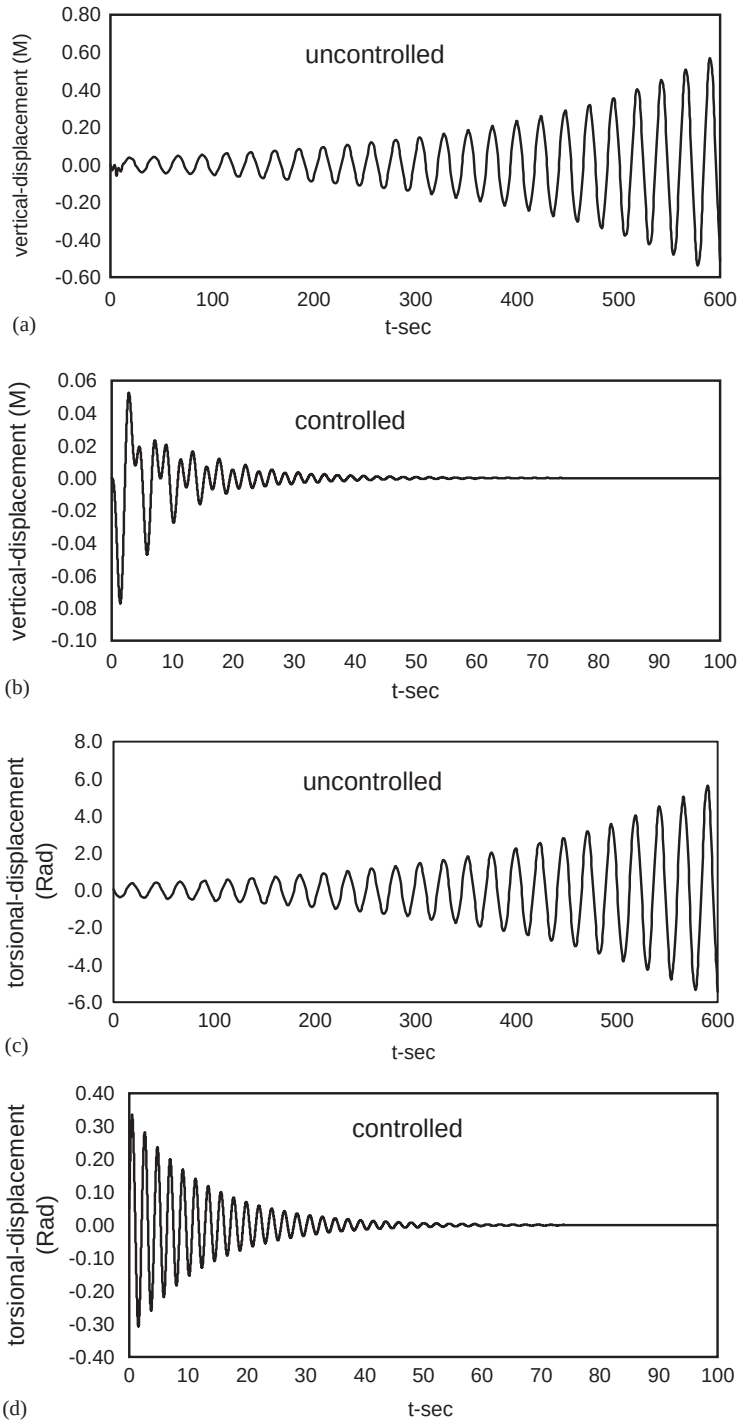

Fig. 10. Controlled and uncontrolled bridge responses due to initial conditions at mean wind speed $U = 60\,\mathrm{m/s}$.

Table 3
State feedback gain matrix $[\mathbf{K}_1]$ and observer gain matrix $[\mathbf{K}_e]$ for different cases

Case 1, $U = 50$ (m/s)		Case 2, $U = U_f = 55.52$ (m/s)		Case 3, $U = 60$ (m/s)	
State feedback gain matrix $[\mathbf{K}_1]$	Observer gain matrix $[\mathbf{K}_e]$	State feedback gain matrix $[\mathbf{K}_1]$	Observer gain matrix $[\mathbf{K}_e]$	State feedback gain matrix $[\mathbf{K}_1]$	Observer gain matrix $[\mathbf{K}_e]$
0.0448	−22012.00	0.0003	−1946.87	−0.0004	−1712.72
3.5924	−47.67	−0.1300	−77.11	0.2845	−103.02
−0.2376	28585.79	0.0012	28095.86	0.0003	25242.39
−0.2200	−33095.48	0.0065	−23983.13	0.2114	−16972.99
−0.4769	14356.92	−0.0008	2971.71	0.0007	4115.57
−57.3547	−1073.93	−0.0879	−1084.34	0.1028	−1095.45
−0.0725	−1263.37	−0.00007	−22187.15	−0.00006	−37726.37
0.2367	27892.86	0.1599	40143.30	0.1693	43608.88

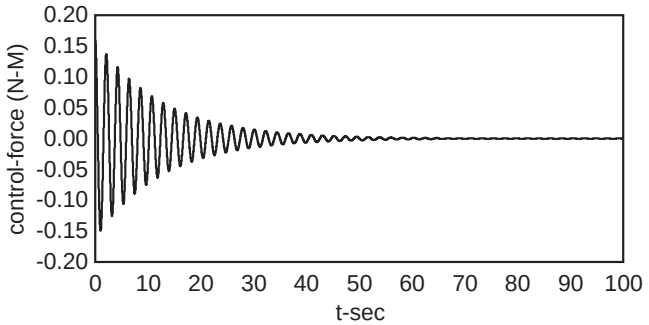

Fig. 11. Control force to reduce the bridge response at mean wind speed $U = U_f = 55.52\,\mathrm{m/s}$.

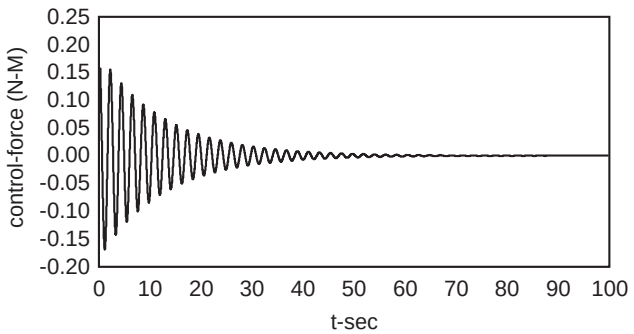

Fig. 12. Control force to reduce the bridge response at mean wind speed $U = 60\,\mathrm{m/s}$.

designing a state feedback gain matrix, which forces the real part of the dominant pole of the system to a desired negative value. The control algorithm performs in conjunction with a full-order state observer. The control strategy is used to increase the flutter wind speed of Vincent

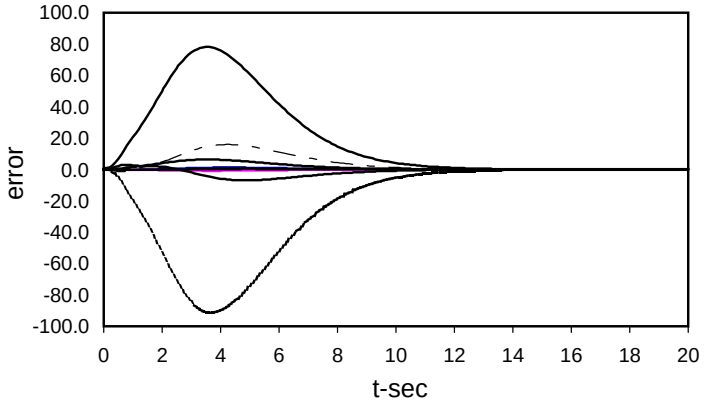

Fig. 13. Variation of the error between the actual state variables and observed state variables.

Thomas Bridge by applying an active torsional moment at the middle of its center span. Numerical studies on the bridge show that

(i) The proposed control strategy significantly reduces the decay time to bring down the transient response to almost zero value for aerodynamic excitation caused by a wind speed less than the flutter wind speed.
(ii) For wind speed greater than/equal to the flutter wind speed, the divergent/sustained oscillations (respectively) are brought down to about zero value by the control strategy within a decay time of about 50 s.
(iii) The maximum values of the required control force of the three cases are nearly the same and are quite small.

Appendix A

Matrices $[\mathbf{A}^F]$ and $[\mathbf{B}^F]$ can be written as

$$[\mathbf{A}^F] = \begin{bmatrix} H_1^* L_1 & & \text{zeros} & B' H_2^* L_1 & & \text{zeros} \\ & \ddots & & & \ddots & \\ \text{zeros} & & H_1^* L_n & \text{zeros} & & B H_2^* L_n \\ B' A_1^* L_1 & & \text{zeros} & B'^2 A_2^* L_1 & & \text{zeros} \\ & \ddots & & & \ddots & \\ \text{zeros} & & B' A_1^* L_n & \text{zeros} & & B'^2 A_2^* L_n \end{bmatrix}_{(2n \times 2n)} \tag{A.1}$$

and

$$[\mathbf{B}^F] = \begin{bmatrix} \frac{H_4^*}{B'}L_1 & & \text{zeros} & H_3^*L_1 & & \text{zeros} \\ & \ddots & & & \ddots & \\ \text{zeros} & & \frac{H_4^*}{B'}L_n & \text{zeros} & & H_3^*L_n \\ A_4^*L_1 & & \text{zeros} & B'A_3^*L_1 & & \text{zeros} \\ & \ddots & & & \ddots & \\ \text{zeros} & & A_4^*L_n & \text{zeros} & & B'A_3^*L_n \end{bmatrix}_{(2n\times 2n)}. \tag{A.2}$$

References

[1] N.N. Dung, T. Miyata, H. Yamada, Structural control in consideration of flutter response in long span bridges, in: *Proceedings of the Second International Workshop on Structural Control*, Hong Kong, 1996, pp. 152–162.

[2] N.N. Dung, T. Miyata, H. Yamada, Application of robust control to the flutter in long span bridges, *Journal of Structural Engineering and Earthquake Engineering, JSCE* 42A (1996) 847–853.

[3] M. Gu, C.C. Chang, W. Wu, H.F. Xiang, Increase of critical flutter wind speed of long span bridges using tuned mass damper, *Journal of Wind Engineering and Industrial Aerodynamics* 73 (1998) 111–123.

[4] H. Kobayashi, H. Nagaoka, Active control of flutter of a suspension bridge, *Journal of Wind Engineering and Industrial Aerodynamics* 41–44 (1992) 143–151.

[5] H. Kobayashi, R. Ogawa, S. Taniguchi, Active flutter control of a bridge deck by ailerons, in: T. Kobori, et al. (Eds.), *Proceedings of the Second World Conference on Structural Control*, vol. 3, Kyoto, Japan, 1998, pp. 1841–1848.

[6] Y.Y. Lin, C.M. Cheng, C.H. Lee, A tuned mass damper for suppressing the coupled flexural and torsional buffeting response of long-span bridges, *Journal of Engineering Structures* 22 (2000) 1195–1204.

[7] T. Miyata, H.Yamada, N.N. Dung, K. Kozama, On active control and structural response control of the coupled flutter problem for long span bridges, in: *Proceedings of First World Conference on Structural Control*, vol. 1, Los Angeles, USA, 1994.

[8] J. Nobuto, Y. Fujino, M. Ito, A study on the effectiveness of TMD to suppress a coupled flutter of bridge deck, *Journal of Structural Mechanics and Earthquake Engineering, JSCE* 398 (1–10) (1998) 413–416 (in Japanese).

[9] F. Sakai, S. Takaeda, T. Tamaki, Tuned liquid column damper (TLCD) for cable-stayed bridges, in: *Proceedings Specialty Conference on Innovation in Cable-Stayed Bridges*, Fukuoka, Japan, 1991, pp. 197–205.

[10] K. Wilde, Y. Fujino, T. Kawakami, Analytical and experimental study on passive aerodynamic control of flutter of bridge deck section, *Journal of Wind Engineering and Industrial Aerodynamics* 80 (1–2) (1998) 105–119.

[11] M. Yoneda, Y. Fujino, H. Kande, A. Yamamoto, Y. Miyamoto, O. Ando, K. Maeda, T. Katayama, A practical study of tuned liquid damper with application to the Sakitama Bridge, *Journal of Wind Engineering* 41 (1989) 105–106 (in Japanese).

[12] S. Pourzeynali, T.K. Datta, Control of flutter of suspension bridge deck using TMD, *Wind and Structures* 5 (2002) 407–422.

[13] F. Branceloni, The construction phase and its aerodynamic issues, in: A. Larsen (Ed.), *Aerodynamics of Large Bridges*, A. A. Balkema, Rotterdam, 1992, pp. 17–158.

[14] S. Phongkumsing, K. Wilde, Y. Fujino, Analytical study on flutter suppression by eccentric mass method on 3D full suspension bridge model, in: *Proceedings of the Second World Conference on Structural Control*, vol. 3, Kyoto, Japan, 1998, pp. 1797–1806.

[15] K. Wilde, Y. Fujino, V. Prabis, Effects of eccentric mass on flutter of long span bridge, in: *Proceedings of Second International Workshop on Structural Control*, Hong Kong, 1996, pp. 564–574.
[16] G.W. Housner, L.A. Bergman, T.K. Caughey, A.G. Chsiakos, R.O. Claus, S.F. Masri, R.E. Skelto, T.T. Soong, B.F. Spencer, J.T.P. Yao, Structural control—past, present and future, *Journal of Engineering Mechanics, ASCE* 123 (9) (1998) 897–958.
[17] L. Meirovitch, D. Ghosh, Control of flutter in bridges, *Journal of Engineering Mechanics, ASCE* 113 (5) (1987) 720–736.
[18] R.H. Scanlan, J.G. Beliveau, K.S. Budlong, Indicial aero-dynamic function for bridge deck, *Journal of Engineering Mechanics, ASCE* 100 (EM4) (1974) 657–672.
[19] A. Jain, N.P. Jones, R.H. Scanlan, Coupled flutter and buffeting analysis of long-span bridges, *Journal of Structural Engineering, ASCE* 122 (1996) 716–725.
[20] R.H. Scanlan, J.J. Tomko, Airfoil and bridge deck flutter derivatives, *Journal of the Engineering Mechanics, ASCE* 97 (1971) 1717–1737.
[21] E. Simiu, R.H. Scanlan, *Wind Effects on Structures: An Introduction to Wind Engineering*, Wiley, New York, 1978.
[22] L. Singh, N.P. Jones, R.H. Scalan, O. Lorendeaux, Simultaneous identification of 3-D aeroelastic parameters, in: *Proceedings of the Ninth International Conference on Wind Engineering*, New Delhi, India, 1995.
[23] A.M. Abdel-Ghaffar, Suspension bridge vibration: continuum formulation, *Journal of Engineering Mechanics, ASCE* 108 (1982) 1215–1232.
[24] A.M. Abdel-Ghaffar, Free torsional vibrations of suspension bridges, *Journal of the Structural Engineering, ASCE* 105 (1979) 767–789.
[25] A.M. Abdel-Ghaffar, Vertical vibration analysis of suspension bridges, *Journal of the Structural Engineering, ASCE* 106 (1980) 2053–2074.
[26] K. Ogata, *Modern Control Engineering*, Prentice-Hall of India, New Delhi, 1997.
[27] U. Aldemir, M. Bakioglu, Active structural control based on the prediction and degree of stability, *Journal of Sound and Vibration* 247 (7) (2001) 561–576.
[28] U. Aldemir, Modified disturbance rejection problem, *Computers and Structures* 81 (2003) 1547–1553.
[29] K. Ogata, *Discrete-time Control System*, Prentice-Hall, Upper Saddle River, NJ, 1995.